Ring Attractor Dynamics of Head Direction Representation

Pantong Yao
Department of Neurosciences
University of California, San Diego
San Diego , CA 92161
p1yao@ucsd.edu

Jessica Du
Department of Neurosciences
University of California, San Diego
San Diego , CA 92161
j4du@ucsd.edu

Abstract

Ring attractors are a class of recurrent networks schematized as a ring of neurons whose connectivity depends on their tuning preferences. They have been used to model various circuits in the brain, most notably cells that encode head direction. A ring attractor sustains a bump-like activity pattern with infinite time constant, which can be updated by external input and internal dynamics. For head direction cells, a ring attractor circuit would stably represent the current head direction, with peak activity changing in response to inputs from the vestibular system describing angular head velocity. We constructed different models for head direction cells, including ring attractor models, using several distinct network structures and explored their dynamics.

1 Introduction

Head direction cells in the central nervous system fire whenever the animals faces towards a particular direction and therefore maintain an internal representation of the head direction. A good head direction representation system must satisfy several requirements: 1) It must be unique as an animal can face only one direction at a given time; 2) it has to be persistent since animals can internally keep track of their head direction without external sensory input (for example in total darkness); 3) and it must allow updating that matches the heading changes expected from the animal's movements (Seelig and Jayaraman 2015, Kim, Rouault et al. 2017). Ring attractors are a class of recurrent networks made up of neurons with orientation tuning, meaning that they fire to represent a specific preferred orientation. These neurons are arranged in an abstract ring of orientations, and form connections with each other based on the relationship between their preferred orientations. Ring attractors have been proposed as a network structure underlying the mechanism of head direction representation in the brain (Knierim and Zhang 2012). In this project, we simulated a ring attractor model for head representation and tested whether the model can recapitulate the three key features of the head direction representation system.

2 Methods

2.1 Simulation of the symmetric ring attractor

2.1.1 Design of the symmetric ring model

We first considered a one-dimensional attractor network consisting of 500 of neurons whose preferred angle ϕ are uniformly distributed on $[0,\ 2\pi)$. The connectivity between each pair of neurons (any neurons i and j) was given by:

Preprint. Under review.

$$W_{ij} = W_0 \left(\cos(\phi_i - \phi_j) - \frac{1}{2} \right) \tag{1}$$

$$\tag{2}$$

As a result, neurons activate other neurons with similar preferred angle and inhibit neurons with dissimilar preferred angle (Fig. 1).

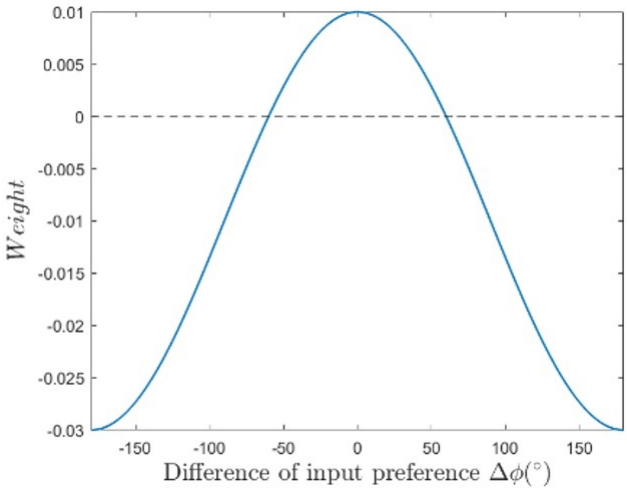

Figure 1: *Rate functions over different voltages*

2.1.2 Dynamic equation for spontaneous activity

The spontaneous activity of the ring model was given by the differential equation:

$$\tau \frac{dr_i}{dt} = -r_i + \mathcal{F}\left(\sum_{j=1}^{N} W_{ij} r_j \right) \tag{3}$$

$$\tag{4}$$

For our simulation, we defined the non-linearity F as a hyperbolic tangent function:

$$\mathcal{F}(x) = \frac{1 \ + \tanh(x)}{2} \tag{5}$$

$$\tag{6}$$

The network state $\vec{r}$ was randomly initialized in order to break the symmetry:

$$r_i \sim Unif\ [0, 10^{-8}] \tag{7}$$

$$\tag{8}$$

2.1.3 Dynamic equation for evoked activity

To simulate the evoked response of the network to inputs, we introduced the term $I_i(t)$ to represent the input current for and individual neuron. Thus, the activity of the ring model was modified as:

$$\tau \frac{dr_i}{dt} = -r_i + \mathcal{F}\left(I_i + \sum_{j=1}^{N} W_{ij} r_j\right) \tag{9}$$

$$\tag{10}$$

Due to the tuning properties that emerge from the feedforward network, an input representing the head direction ϕ_0 will not only provide input current to the neuron with preferred orientation ϕ_0, but also neurons that have angular preference close to ϕ_0. We represented the input current felt by each neuron i with preferred orientation ϕ_i due to an input representing ϕ_0 using the following equation:

$$I_i = \frac{K^{\cos(\phi_i - \phi_0)}}{K} \tag{11}$$

$$\tag{12}$$

where K is a constant controlling the width of the function. For our simulations we set $K = 100$. This creates an input function reminiscent of psychometric tuning curves (Fig.2).

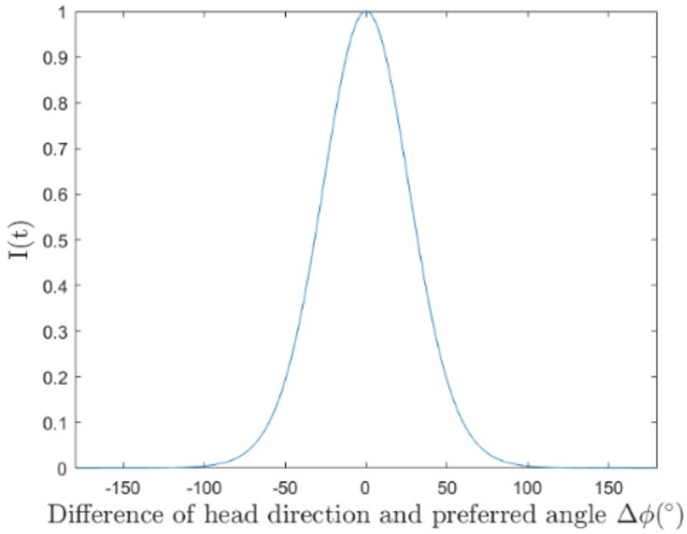

Figure 2: *Input current to an individual neuron as a function of the difference between input head direction and preferred orientation of the neuron*

2.2 Simulation of the asymmetric ring attractor

2.2.1 Design of the asymmetric ring model

The head direction system can track the animal's head direction based on the rotational speed of the head, without external sensory input. To achieve that, we must introduce an asymmetric connectivity matrix to the ring model and generate limit cycle behavior. For the asymmetric ring model, we used the following to describe connectivity between every pair of neurons i and i:

$$W_{ij} = W_0 \left(\cos(\phi_i - \phi_j - \phi_{bias}) - \frac{1}{2}\right) \tag{13}$$

$$\tag{14}$$

where ϕ_{bias} is a bias term that shifts the maximum synaptic connectivity to several neurons away from itself (Fig. 3).

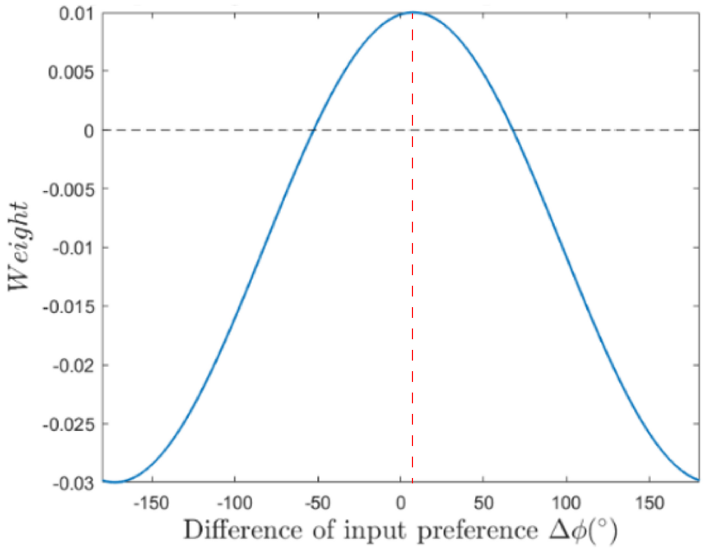

Figure 3: *Shifted synaptic connections in the asymmetric ring model*

2.2.2 Dynamic equation for angular velocity modulation

The rotation speed of the ring must be determined by the angular velocity of the head, ω_{head}. Although it might be possible to modulate the ring rotation speed by adjusting ϕ_{bias} based on ω_{head}, this is unlikely to the be a mechanism used by the biological head direction system due to the slow dynamics of weight updating. Instead, we introduced a multiplicative speed modulation term to the firing rate of the neurons in the model, to make the firing rate proportional to the rotational speed (based on Ocko, Hardcastle et al. 2018):

$$r_i' = \frac{\omega(t)}{\omega_0} r_i \tag{15}$$

$$\tag{16}$$

Then we used r_i' as an input to the original differential equation.

2.3 Simulation of the feedforward model

The feedforward model is a simple network model where neurons in the ring are not interconnected, and derive their orientation selectivity and orientation tuning via their feedforward inputs from other regions. This model has been used in previous studies, but we believe that it does not reflect the key characteristics of the head direction system as well as the ring attractor model. Thus, we used the feedforward model as a comparison to our ring attractor model.

For the feedforward model, we set W_{ij} to be 0 for the pure feedforward model (no connections between neurons in the ring) and used the same dynamic equation and external input described in 2.1.2 - 2.1.3 for the simulation.

3 Results

3.1 The ring attractor generates a persistent activity bump spontaneously

In order to examine whether the ring attractor model can generate the desired dynamics for head direction representation, we first simulated a ring model without any external input (See Method 2.1.1-2.1.2). As expected from our design of the ring model, a spontaneous activity bump was generated at a random position on the ring of neurons (Fig. 4A-B). After the bump was formed, it

stabilized at its position on the ring without any drifting, jumping or change in shape. This result suggests that the ring attractor model can form a bump which can sustain itself without direct external input, which supports a key characteristic of the head direction system.

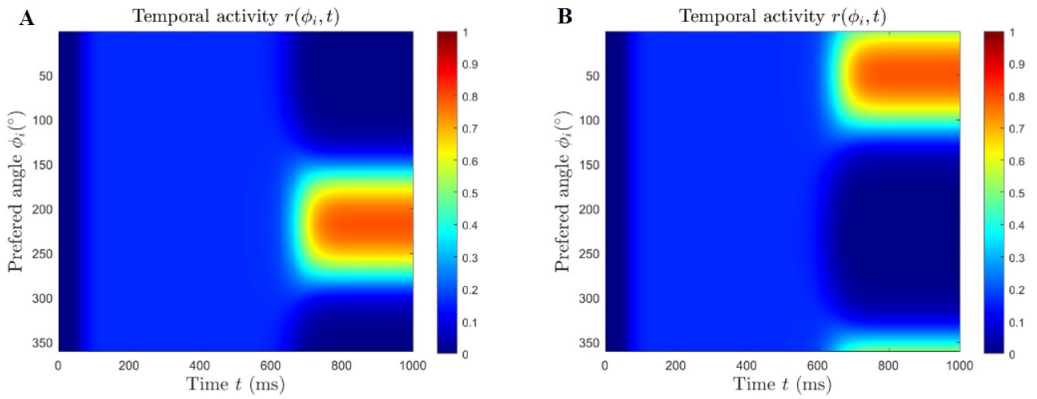

Figure 4: *Spontaneous activity bump generated by the ring model. (A) A spontaneous bump centered at a neuron with a preferred orientation of 220; (B) A spontaneous bump centered at a neuron with a preferred orientation of 50.*

3.2 The bump position can be updated by direct external input

After the bump was generated, we introduced a time-varying external input to test whether the activity bump can be updated by external input (Fig. 5A,C). After the onset of stimulation (at the first white line), the bump slowly drifted towards the external input angle instead of jumping onto it directly (fig. 5B); the bump always exists continuously. After we withdraw the external stimulation, the activity bump of the ring model stayed at the its position. This is in contrast to the feedforward model. The feedforward model did not generate a spontaneous bump, and while it did form one upon stimulation onset, this bump would disappear and reform when the input orientation changed. Also, the bump of the feedforward model faded away when we withdrew stimulation.

These results suggest that the ring model can track external input and the maintain activity without input, which satisfies the requirements of persistence and updatability for the head direction representation. The ring model reflects these characteristics better than the pure feedforward model.

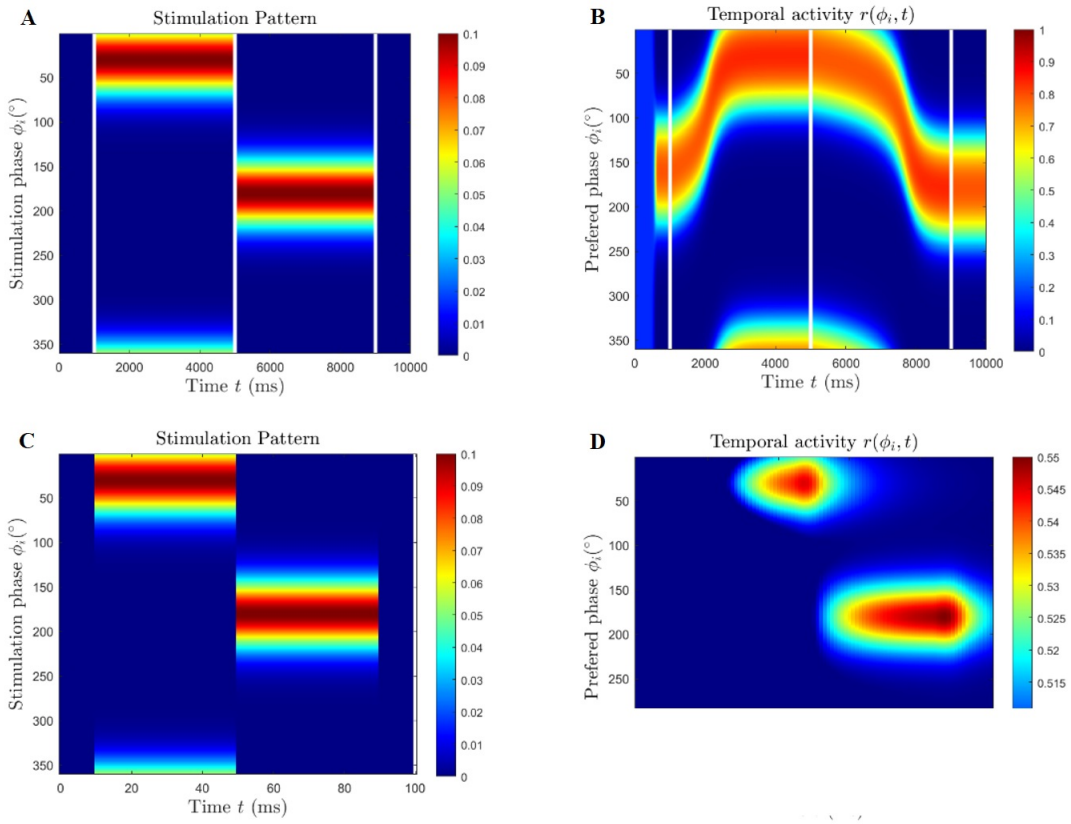

Figure 5: *The activity bump of the ring model moves towards external input. (A) The stimulation pattern of the external input to the ring model; (B) The bump of the ring model moves gradually towards the external input angle and persists after stimulation ends. (C) The stimulation pattern of the external input to the pure feedforward model; (D) The bump of the feedforward model jumps in response to changes in the external input angle, and disappears when stimulation ends.*

3.3 The bump is unique even with conflicting external input

To check the uniqueness of the bump on the neuronal ring, we introduced two conflicting external input (Fig. 6A, C). The feedforward showed two bumps in response to the two input angles (Fig. 6D). However, the bump of the ring model converged to one of the input angles (Fig. 6B), offering a unique representation for head direction.

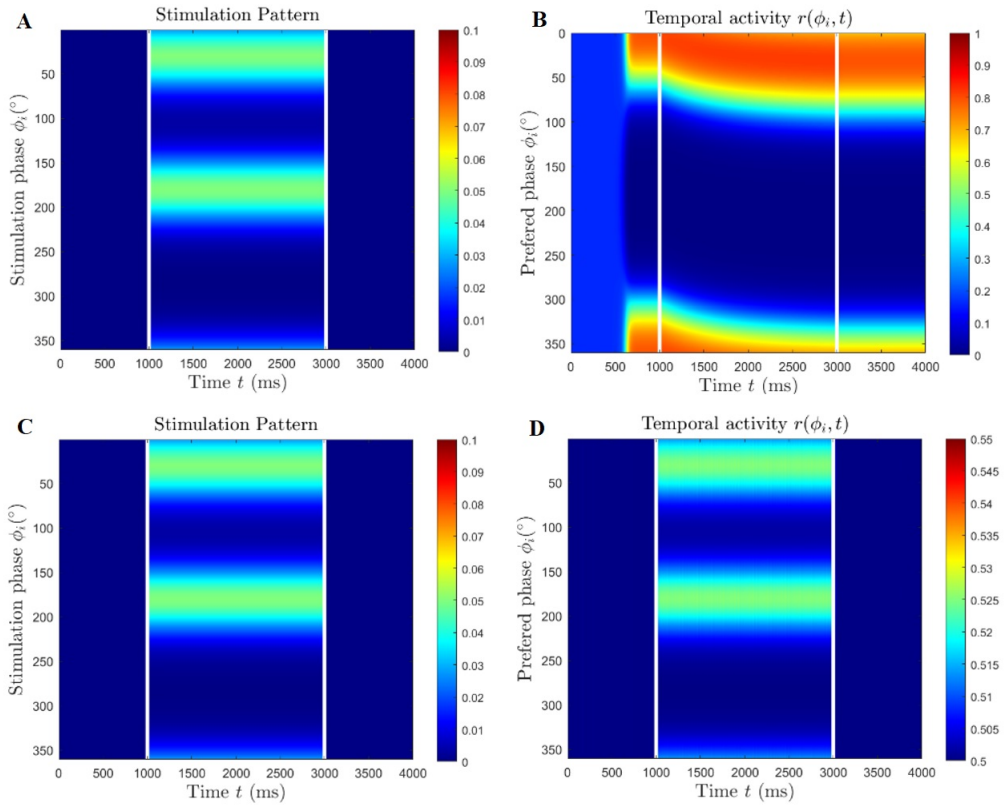

Figure 6: *The uniqueness of the bump in the ring model. (A) The stimulation pattern of the external input to the ring model; (B) The bump of the ring model moves towards one of the external input angle and remains unique. (C) The stimulation pattern of the external input to the pure feedforward model; (D) The bump of the feedforward model was split.*

3.4 The bump can be updated based on the internal representation of angular velocity

When we close our eyes and rotate our heads, we can still keep track of our head direction. This is because our internal representation of head direction can be updated based on inputs from the vestibular system describing head angular velocity (Turner-Evans, Wegener et al. 2017). To achieve this in our model, we modified the ring attractor to make it rotate as a limit cycle (See Method 2.2). Without any directed head direction input, the activity bump can drift by itself (Fig. 7A). The rotation speed of the bump can then be modulated by the head angular velocity (fig. 7B).

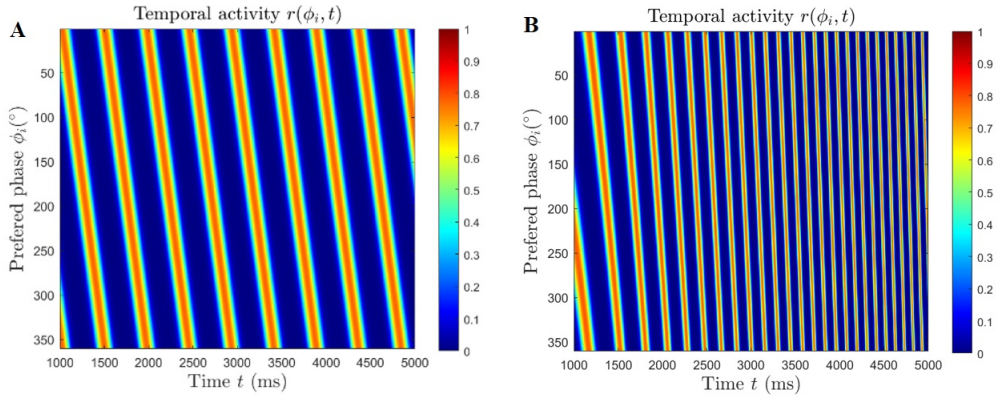

Figure 7: *Rotating the bump without direct head direction input. (A) The bump rotates at a steady rate based on a constant angular velocity input; (B) The bump rotates based on an angular velocity input which is linearly increasing with time.*

3.5 The bump can (to some extent) tolerate mismatch between the angular velocity representation and direct external input

Although we can keep track of head direction with our eyes closed while rotating, we may still lose track if we rotate too many cycles. This might due to a mismatch between the real angular velocity and our internal representation. One consequence of this is that the bump's rotation based on the internal velocity representation may not be able to match direct external head direction input. However, it seems we never feel this mismatch in our daily life when we have both the direction input and the velocity input. In the next part, we explored what would happen to the ring model if we have a mismatch between direction input and velocity input (Campbell, Ocko et al. 2018). For simplicity, in all of the following simulations, we kept the internal velocity representation as a constant, and increased or decrease the real angular velocity.

First, we slowed down the rotation speed of the direct input, which means the internal representation of the angular velocity is faster than the real one (Fig. 8A). Before the external input onset, the ring rotates based on the internal velocity representation (Fig. 8B, 1000 – 3000 ms). After direct external input was introduced, the bump on the neuron ring starts to follow the external input (fig. 8B, 3000 – 6000 ms), such that the steady-state phase difference between the external input and the peak position on the neuronal ring quickly becomes negligible (Fig. 8C, 3000 – 6000 ms).

As we slow the external input further, the rotation speed of the neuronal ring further slows down to track the external input(Fig. 8C, 6000 – 9000 ms). However, the steady-state phase difference increased slightly in this case (Fig. 8C, 6000 – 9000 ms). After we withdrew the external input, the bump went back to its original internal rotation speed (Fig. 8B, 9000 – 10000 ms).

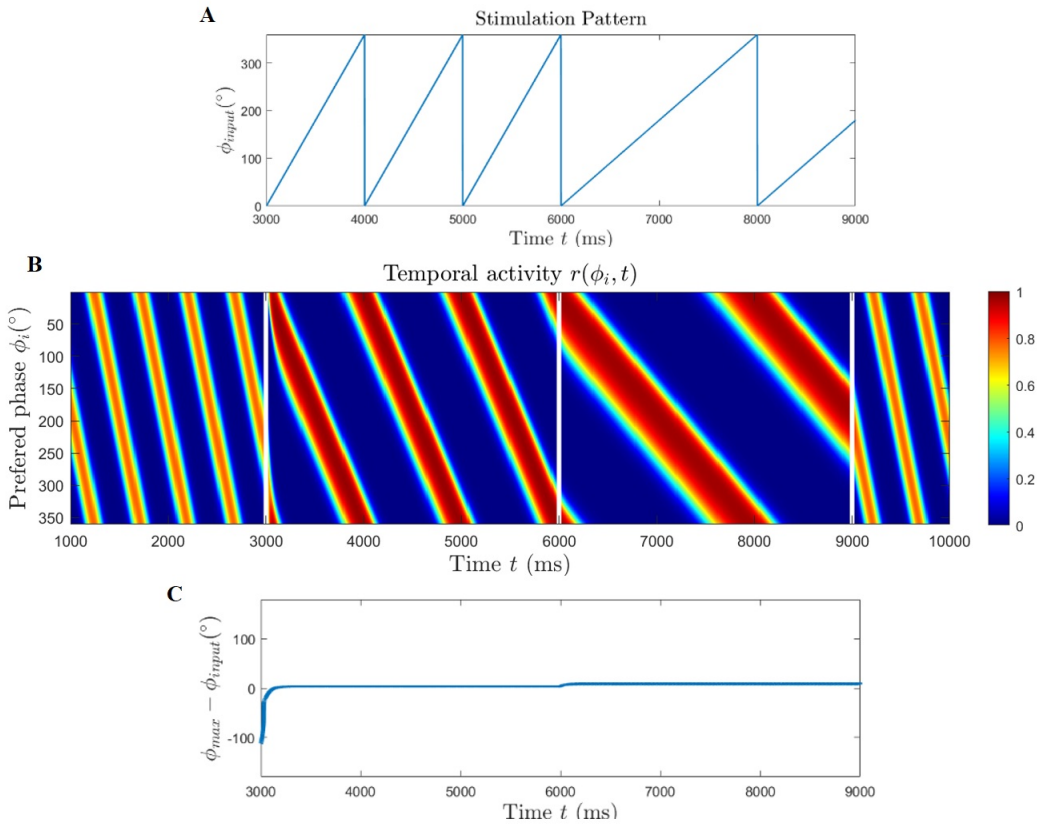

Figure 8: *The bump can tolerate mismatch between the angular velocity representation and direct external input when the internal representation of the angular velocity is faster than the external input (A) The external head direction input angle; (B) The bump rotates and responds to the external head direction input and internal velocity input; (C) The phase difference between the external input angle and the peak position on the neuronal ring*

Next, we speed up the rotation of the direct input, which means the internal representation of the angular velocity is now slower than the real one (Fig. 9A). The bump on the ring can still follow the external input when there is a mild mismatch (Fig. 8B, 3000 – 6000 ms). This is reflected in the steady-state phase difference between the external input and the bump peak position, which is negligible during this period (Fig. 8B, 3500 – 6000 ms).

When we sped up the external input even further, the rotation speed of the activity bump was unable to follow the external input (Fig. 9B, 6000 – 9000 ms). The steady-state phase difference between the external input and the bump peak position is quite significant (Fig. 9C, 6000 – 9000 ms).

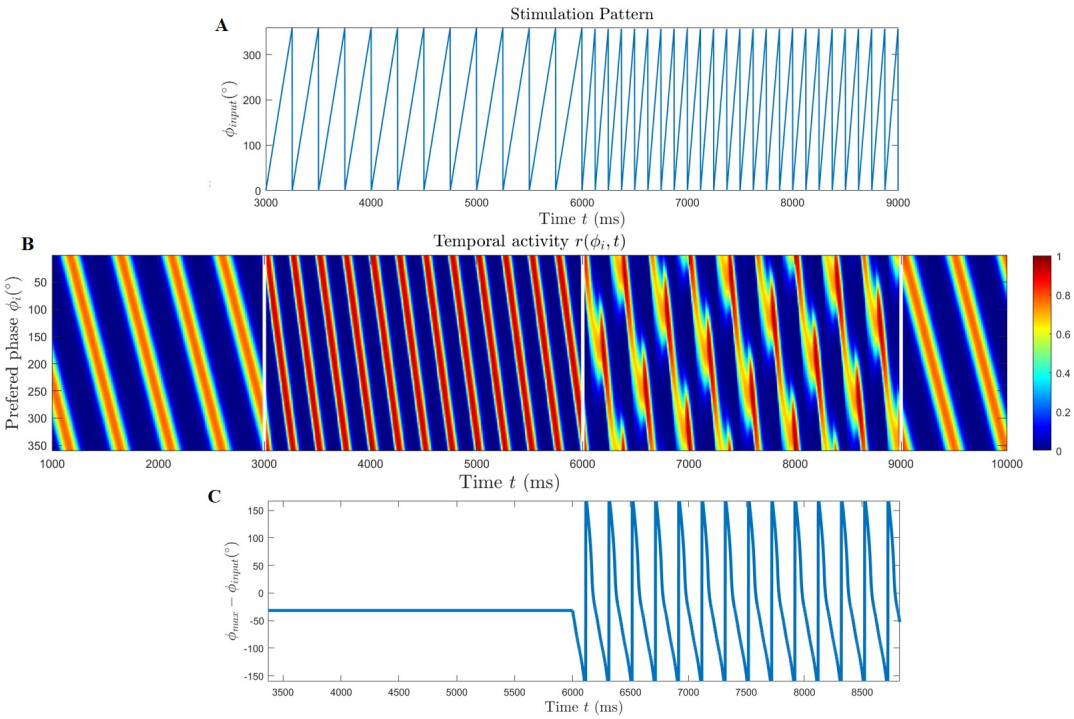

Figure 9: *The bump can to some extent tolerate the mismatching of the angular velocity representation and direct external input; here is a case when the internal representation of the angular velocity is too slow. (A) The external head direction input angle; (B) The bump rotates to reflect the external head direction input and internal velocity input; (C) The phase difference of the external input angle and the peak position on the neuronal ring*

4 Discussion

In this project, we simulated a ring attractor model and explored its dynamic properties. We found the ring attractor can generate a bump spontaneously (Fig. 1,4), and the bump will drift to match the external head direction input (fig. 2,5). We found the bump was stable even without external input and it was always unique even with multiple external inputs (Fig. 4-6). By connecting the neurons asymmetrically, we made the bump rotate based on the internal angular velocity representation without head direction input (Fig. 3,7). And finally, we explored the tolerance of ring attractor to mismatches between the internal angular velocity representation without head direction input (Fig. 8,9).

Because of the many desirable properties of the ring attractor, it has also been used to model other representation systems for 1-D variables without boundary, such as orientation tuning in visual cortex (Ben-Yishai et al. 1995, Somers et al. 1995, Ferster Miller 2000). The ring attractor can be further extended to 2-D as a torus attractor for modelling the 2-D grid cell pattern (Campbell, Ocko et al. 2018). More recently, others have hypothesized a persistent working memory model that relies on the self-sustainable property of the ring attractor (Bouchacourt and Buschman 2019). In addition, it may be possible in the future to implement the ring model as an network structure for artificial recurrent neural networks.

5 Conclusions

The dynamics of the ring attractor may underlie the mechanisms for head direction representation in biological systems. In support of this, we have shown that it satisfies the three key feature of the head direction representation: 1) it represents the current head direction stably even without direct external

input, 2) it integrates both the direct head direction inputs and the internal angular head velocity representation, and 3) it maintains the uniqueness of the head direction even with conflicting inputs.

6 References

[1] Ben-Yishai R, Lev Bar-Or R, Sompolinsky H (1995). "Theory of orientation tuning in visual cortex". Proc Natl Acad Sci U S A 92:3844–8.

[2] Bouchacourt, F. and T. J. Buschman (2019). "A Flexible Model of Working Memory." Neuron 103(1): 147-160 e148.

[3] Campbell, M. G., S. A. Ocko, C. S. Mallory, I. I. C. Low, S. Ganguli and L. M. Giocomo (2018). "Principles governing the integration of landmark and self-motion cues in entorhinal cortical codes for navigation." Nat Neurosci 21(8): 1096-1106.

[4] Ferster D, Miller KD (2000). "Neural Mechanisms of Orientation Selectivity in the Visual Cortex". Annu Rev Neurosci 23:441–71.

[5] Kim, S. S., H. Rouault, S. Druckmann and V. Jayaraman (2017). "Ring attractor dynamics in the Drosophila central brain." Science 356(6340): 849-853.

[6] Knierim, J. J. and K. Zhang (2012). "Attractor dynamics of spatially correlated neural activity in the limbic system." Annu Rev Neurosci 35: 267-285.

[7] Ocko, S. A., K. Hardcastle, L. M. Giocomo and S. Ganguli (2018). "Emergent elasticity in the neural code for space." Proc Natl Acad Sci U S A 115(50): E11798-E11806.

[8] Seelig, J. D. and V. Jayaraman (2015). "Neural dynamics for landmark orientation and angular path integration." Nature 521(7551): 186-191.

[9] Somers DC, Nelson SB, Sur M (1995). "An emergent model of orientation selectivity in cat visual cortical simple cells". J Neurosci 15:5448–65.

[10] Turner-Evans, D., S. Wegener, H. Rouault, R. Franconville, T. Wolff, J. D. Seelig, S. Druckmann and V. Jayaraman (2017). "Angular velocity integration in a fly heading circuit." Elife 6.